Testing Our Understanding of Short Period Mass Variation Processes with Future Earth Gravity Missions

K. Kang[1] and P. L. Bender[2]

[1]Department of Physics, University of Colorado Boulder, 390 UCB, Boulder, CO, 80309-0390, USA

[2]JILA, University of Colorado Boulder and NIST, 440 UCB, Boulder, CO, 80309-0440, USA

Key Points:

- The acceleration noise in future Earth gravity variation missions can be much reduced by using simplified Gravitational Reference Sensors
- With low measurement noise, short wavelength variations in the geopotential height can be measured from individual short arcs of data
- 30-day or shorter global average solutions for geopotential variations will be improved, but will still be affected by temporal averaging

Corresponding author: Peter L. Bender, pbender@jila.colorado.edu

Abstract

A new mission called GRACE Follow-On is now flying to continue the measurements started by the GRACE mission, and to test a laser interferometry system for making more accurate measurements of the satellite separation. In this paper we discuss the potential scientific benefit of strongly reducing the acceleration noise in a Next Generation Gravity Mission (NGGM), compared with that for GRACE and for GRACE Follow-On. A useful way of comparing the scientific benefits is from the view point of how well they can be used to test different procedures for estimating the changes in the geopotential based on sources of geophysical information other than satellite gravity results. In particular, changes in hydrology, the atmospheric density, and ocean conditions can make large and very non-uniform changes in the geopotential in short periods of time. To make the discussion as simple as possible, we consider mainly the variations in the geopotential at altitude along the satellite orbit for different ground tracks. For the NGGM, we initially assume laser interferometry between the two satellites but the same satellite acceleration noise level as for the GRACE-Follow-On mission. Then the total measurement noise level at long and medium wavelengths would be only moderately below the geopotential variation estimation uncertainty. However, if the acceleration noise level were sharply reduced by replacing the GRACE-type accelerometers by simplified gravitational reference sensors, it appears that considerably improved tests of different procedures for geophysical estimates of the geopotential variations could be made.

1 Introduction

Satellite measurements of the Earth's time-variable gravity field are capable of addressing a wide variety of geophysical problems, such as the mass redistributions caused by hydrology, oceanography, the cryosphere, and the solid Earth. GRACE (the Gravity Recovery And Climate Change Experiment) provided regular monthly estimates of the Earth's gravity field from when it was launched in 2002 (Tapley et al., 2004) until 2017 (Tapley et al., 2019). The monthly average gravity fields were given in terms of the Stokes coefficients up to degree 120, and they have been used successfully in extensive studies of changes in continental water storage, ice sheet mass, and sea level, as well as for earthquake-related deformation monitoring (Watkins et al., 2015).

Time variations in the Earth's mass distribution over periods of hours and longer are being monitored in many different ways. The results from the GRACE mission have

been very valuable, but the changes in the geopotential during the usual global averaging time of about a month make it difficult to determine changes at particular locations at shorter periods. This limitation is called temporal aliasing. The satellites do not monitor the entire global field continually during a month, but sample the gravity field only along their orbital track. The resulting infrequent sampling of the signal leads to the aliasing of short period variations into the monthly averages (see e.g., Han, 2004). For example, the short period temporal mass variations alias into the longer period components and systematically contaminate the monthly mean gravity field estimates (see e.g., Han et al., 2006). The usual way to reduce these aliasing errors is to independently model and remove the effects of the various types of sub-monthly gravity variations before constructing monthly averages. But errors in these short period gravity variation models will cause aliasing errors in the monthly gravity field solutions.

The main objective of the recently launched GRACE Follow-On Mission (GRACE-FO) is to continue the roughly monthly determinations of variations in the global gravity field that were started by the GRACE mission (Landerer et al., 2020). However, GRACE-FO also carries a laser ranging interferometer (LRI) as a demonstration experiment (Kornfeld et al., 2019). The LRI measures changes in the satellite separation with extremely high accuracy. GRACE basically used microwave measurements to determine changes in the satellite separation with an accuracy of about 1 micron/($\mathrm{Hz}^{0.5}$). However, the initial operation of the LRI on GRACE-FO has shown a much lower noise level (Abich et al., 2019). If this performance continues during the rest of the GRACE-FO mission, the results will be used by many groups to determine more accurately the global distribution of geopotential heights for roughly 30 day periods. But it is known that the percentage improvement in the accuracy for the global solutions will be limited considerably by temporal aliasing (see e.g., Flechtner et al., 2016).

To improve our understanding of the effects of various types of mass distribution changes on time variations in the Earth's geopotential, the consideration of changes in the global averages over periods of up to 30 days will continue to be the main approach that is used. However, for testing our understanding of how the changes are occurring, observing the geopotential changes along individual arcs also is expected to be valuable. This approach has been emphasized recently and put on a more rigorous basis by Ghobadi-Far et al. (2018).

A measure of our understanding is how well we can go from observed changes in quantities like the local rainfall, evapotranspiration, and runoff to changes in the mass distribution and therefore the local geopotential. If different procedures for estimating the geopotential changes along a particular arc for GRACE-type missions can be compared directly with observations, the full use can be made of the accuracy of the observational data to evaluate the different procedures. This approach of comparing different estimation procedures along particular arcs reduces the limitations from temporal aliasing on comparing different procedures.

There are two quite well known approximation procedures for carrying out determinations of the geopotential variations along individual arcs. One is based on the conservation of energy for each satellite (Jekeli, 1999, 2017) and the other on the acceleration difference between the two satellites (Weigelt, 2017; Ghobadi-Far et al., 2018). To keep the discussion as simple as possible, we have used just the leading term in a series of terms given in eq. 29 of Jekeli (1999). This approximation was introduced by Wolff (1969) in the same paper where the basic idea of low-low satellite-to-satellite ranging was proposed. It also has been used by a number of other authors. Either the energy conservation approach or the acceleration difference approach has been used in a number of papers where the observed geopotential variations along individual orbital arcs are used in regional or global studies of time variations in the geopotential. (See e.g., Han et al., 2005; Ghobadi-Far et al., 2018).

The formula we have used for the geopotential variations is given by eq. 23 of Jekeli (1999):

$$V_{12} \approx |\dot{x}|(\dot{\rho}_{1,2}). \tag{1}$$

The geopotential energy for each satellite is taken to approach zero at large distances from the Earth, and thus is negative at closer distances. Here V_{12} varies as the difference in potential energy between the two satellites, $|\dot{x}|$ is the mean velocity of the two satellites along the first axis of a local coordinate system, and $\dot{\rho}_{1,2}$ is the projection of the velocity difference between the satellites onto the line joining them. There have been a number of studies to try to evaluate how accurate this approximation or more detailed ones are likely to be in GRACE type missions, and the general conclusion is that the dominant part of the error in most cases will be at the lower orbital frequencies, such as 20 cycles/rev or below. However, as the accuracy for measuring the satellite separation im-

proves, and if the acceleration noise also is substantially reduced, it is not yet known if this will continue to be the case. Further studies are needed in order to determine how much uncertainties such as those in the satellite orbits or the satellite attitude will affect the apparent Fourier amplitudes of geopotential variations at the higher frequencies.

As an over-simplified example of how the conservation of energy approximation works, assume that the Earth's mass distribution is nearly spherically symmetric, but that there is a small masscon at one location. The geopotential height at satellite altitude will then have a small dip at this location. A satellite in a nearly circular orbit crossing above the masscon will have an increase in its velocity as it approaches the masscon, and then slow down again afterwards. The same will happen for a second satellite on the same orbit, and behind the first one, but this will happen at a somewhat later time. Thus the relative velocity between the satellites will first increase and then decrease again, after both satellites have passed the masscon. Thus the amplitude and width of the geoptential bump can be determined from the changes in the satellite separation, if no other sources of acceleration are present.

In this paper, we will first present the model we will use as a rough estimate of the uncertainty in geophysical measure of variations in the geopotential at the present time. Then, the measurement uncertainties for a potential NGGM will be discussed, both with the acceleration noise level of GRACE-FO and with the assumption of a much reduced acceleration noise level. Such a reduction can be achieved by replacing the accelerometers on GRACE-FO by simplified versions of the gravitational reference sensors flown on the LISA Pathfinder Mission (LPF mission). This mission was flown in 2017–2018 with ESA as the lead agency. The purpose was to test how well carefully shielded test masses (gravitational reference masses) could be protected from disturbances in a planned future low-frequency gravitational wave mission called LISA. The results from the LPF mission, Armano et al. (2018), will be discussed in Section 5.

In both cases, the noise level in measuring the variations in the satellite separation is assumed to be similar to that achieved by laser interferometry on the GRACE-FO mission. For the higher acceleration noise level, the measurement uncertainty would be only moderately lower than the present geopotential variation uncertainty at frequencies up to about 40 cycles/rev, and then be higher. However, with the strongly reduced accel-

eration noise level, tests of different procedures for obtaining geophysical estimates of the geopotential variations could be carried out at levels below the level of the present uncertainties in the variation estimates up to about 80 cycles/rev..

2 Estimation Error for Mass Variations due to the Atmosphere, the Oceans, and Hydrology

A recent synthetic Earth System Model (ESM) generated by the GeoForschungsZentrum (Dobslaw et al., 2015) is now available, which is based on realistic mass variability in the atmosphere and oceans, and in terrestrial water storage, continental ice-sheets, and the solid Earth. This model is provided in terms of the gravity anomaly potential from these five separate mass variation components, in terms of Stokes coefficients up to degree and order 180. The listed variations include both those expected from present procedures based on other geophysical observations and contributions from random variations. In the ESM, most of the mass variations at medium and short periods are due to the Atmospheric (A), Oceanic (O), and Terrestrial Water Storage (H) components. For the atmospheric mass variability (A), the updated ESM provides a realistically perturbed de-aliasing model, based on a reanalysis of results from the ECMWF and ERA-Interim studies, which were based mainly on atmospheric density, temperature, and wind velocity data at many sites. However, only a few sites in oceanic areas were available. The oceanic part of the updated ESM, (O), is essentially the sum of three different contributions: the Ocean Model for Circulation and Tides (OMCT); the meso-scale variability not simulated by OMCT; and a uniform variation of sea level in order to keep the total mass in the Earth system constant. For the terrestrial water storage component (H), the best information available from local data on rainfall, evaporation rate, and run-off was used, but the accuracy of the resulting values is fairly uncertain. The temporal resolution for the ESM is 6h and the time period covered is 1995–2006.

In addition to the atmosphere and ocean mass variation models above, a series called AOerr giving estimates of the true uncertainties in A + O has been developed (Dobslaw et al., 2016). It is based on the sum of both large-scale and small-scale errors with zero mean and stationary variance from the updated ESM. We will use the AOerr model to estimate the geopotential height uncertainties along track caused by the present level of uncertainty in procedures for estimating the effects of the atmospheric and oceanic mass variations.

The situation concerning the geopotential variations due to hydrology is more complicated. The effects of continental surface water changes in the updated ESM are built on the basis of the Land Surface Discharge Model (LSDM), which includes the representation of soil moisture, snow storage, and water stored in wetlands, rivers, and lakes (Dill, 2008). There is no error estimate included for the uncertainty in the hydrological model used in the updated ESM. Also, the uncertainty in the accuracy of the input data is even harder to assess than the accuracy of the atmospheric and ocean model results described above. Due to the lack of globally distributed water storage measurements, the LSDM can only be validated indirectly via modelled river discharges and in-situ river discharge measurements. Dill (2008) concluded that the LSDM underestimated the river discharges at low latitudes up to 150% relative to the measurements in regions like the Amazon or Congo basins (from Figure 13 in Dill, 2008). Also, rivers characterized by high evaporation rates and extensive human water consumption, like the Murray River in Australia, are represented insufficiently.However, for comparison purposes, some calculations were done for the H data set from the Earth System Model, as well as for the AOerr data set.

3 Estimate of the Geopotential Variation Uncertainty Along Track

As discussed earlier, for missions similar to GRACE and GRACE-FO, the measurements of variations in the separation between the two satellites can be used to solve for variations in the geopotential height at satellite altitude. For example, the acceleration difference approach with along track analysis is described in Section 2.1 of the paper by Ghobadi-Far et al. (2018) that was mentioned earlier. There a simulation result is given for one case at 500 km altitude which shows that the approximation is quite accurate except for low frequencies, below about 10 cycles/rev. Similar results in papers by Ditmar and van Eck van der Sluis (2019) and by Weigelt (2017) are referred to. Thus we expect that the results we report in the rest of this paper will be fairly accurate, except at low frequencies. However, this will need to be checked by additional studies.

In order to compare the geopotential variation uncertainty along track with the effect of noise in measuring variations in the satellite separation, we have chosen to consider 13-day repeat polar orbits at an altitude of 489 km as possible orbits for the NGGM satellites. For this altitude the orbital rate is 15.23 revolutions/day. To keep the results simple to interpret, we have just included results on four dates for the 2nd, 4th, and 6th

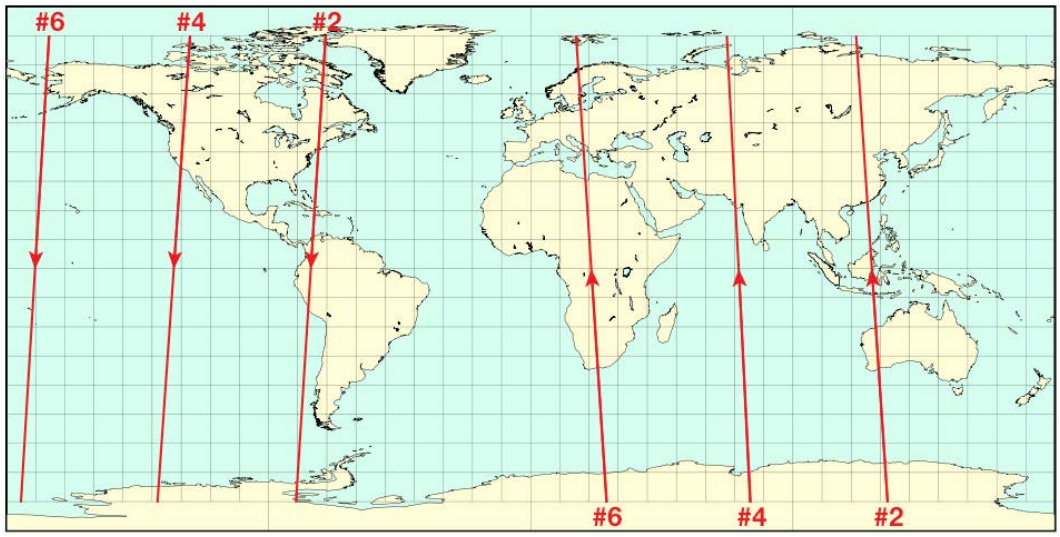

Figure 1. GRACE Follow-On One Revolution Ground Tracks

one revolution arcs that are segments of a single 6 revolution arc, with its first upward zero latitude crossing at 140° E longitude. The geometry of these arcs is shown in Figure 1. The 2nd one rev. arc goes upward across western Australia, Borneo, and eastern Asia, and downward across the western part of South America. The 4th one rev. arc crosses western Asia on its upward path and western Canada and the U. S. on its downward path, with mostly ocean coverage at latitudes below 30° N. The 6th one rev. arc goes upward from the southern tip of Africa to northern Norway, and then downward almost completely across ocean. Thus these three single revolution arcs cover quite different combinations of land and ocean areas, with the upward portion of the 6thone rev. arc covering the most land area.

Using the AOerr data for the estimated geopotential variations with time and location, we chose four dates on which to do the analysis. These are June 30th, September 30th, and December 30th in 2005, and March 30th in 2006. The three months separations between the dates were chosen to allow for possible differences between different seasons. For each of the 12 one rev. arcs, the geopotential height variations were first calculated for points every 1 deg. along the orbit at the satellite altitude, and then Fourier analyzed. The results are given in Figure 2a and Figure 2b for the 2nd and 4th one-rev. arcs, and in Figure 3a for the 6th one rev. arc. The frequencies along the horizontal axis are given in cycles/rev, with 1 cycle/rev corresponding to 0.177 mHz. The results for the

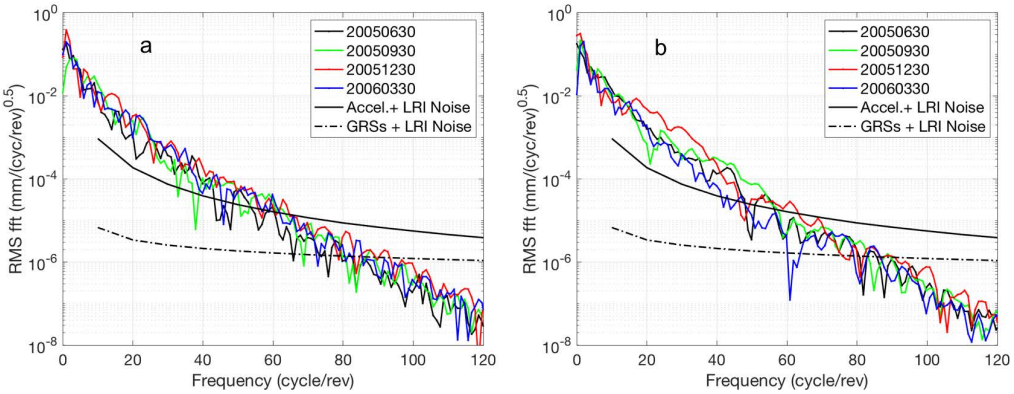

Figure 2. Fourier transform of geopotential height at 490 km along 2nd (a) and 4th (b) arc from AOerr model

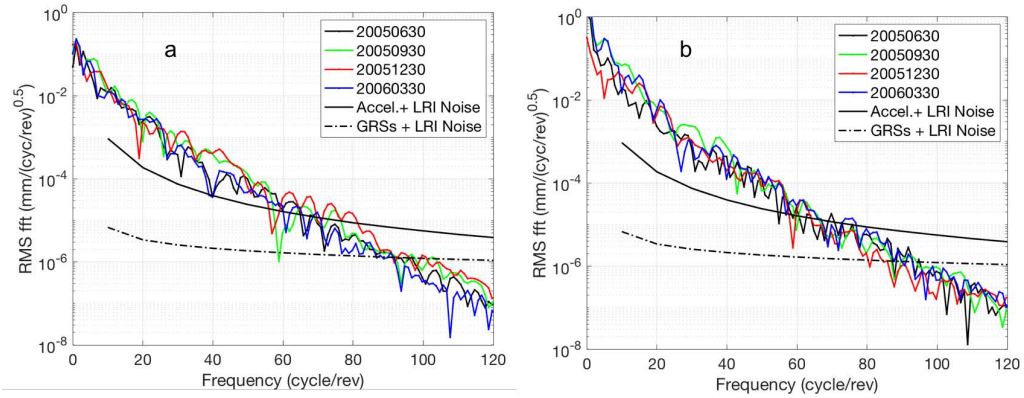

Figure 3. Fourier transform of geopotential height at 490 km along 6th arc from AOerr model (a) and hydrological model (b)

3 arcs are quite similar, despite the quite different land and ocean characteristics for the different arcs.

We also did the calculations for the 6th one rev. arc based on the H data set. The results for the four chosen dates are given in Figure 3b. Perhaps surprisingly, the curves based on the H and AOerr data sets are quite similar along the 6th arc, despite the quite different physical effects involved and sources of the uncertainty in the two data sets.

Also included in Figures 2 and 3 are two curves representing both a high and a low possible instrumental noise curve. These curves are based on different assumptions about the acceleration noise level, as discussed in Section 4, but both assume laser interferometry measurements of changes in the satellite separation.

When we first plotted these curves, we didn't include the Earth's rotation in the analysis. Then, when the Earth's rotation was included, the curves above roughly 90 cycles/rev were quite different. They decreased only something like a factor 3 from 90 cycles/rev to 180 cycles/rev, and were much smoother. The reason was that Fourier analysis assumes that the one rev data set with 1 deg spacing between points would repeat itself for all subsequent one rev arcs, and thus that it can be fit exactly with sine and cosine terms with frequencies from 1 to 180 cycles/rev. The Earth's rotation makes this no longer true, so the Fourier transform program increases the amplitudes for higher frequency terms in order to obtain a better fit to the non-conforming data set. Thus we switched to using a Hahn filter on the data, which corresponds to multiplying the data set by a 1 cycle/rev cosine function that is 0 at the south pole at the start and end of the one rev. arc and at its maximum at the north pole. This made the resulting curves look very much like the ones with no Earth rotation. The Hahn-filtered amplitudes for frequencies up to about 90 cycles/rev were not changed much from those with the rotation but no filtering, so we decided to use them in the rest of this paper.

4 Model for Instrumental Noise

As an alternative in the NGGM design, it has been suggested that the accelerometers be replaced by simplified versions of the gravitational reference sensors (GRSs) flown on the LISA Pathfinder mission (Armano et al., 2018). The performance requirement for the GRSs was 3×10^{-14} m/(s^2)/[(Hz)$^{0.5}$] at frequencies down to 1 mHz, and this performance was exceeded by a factor 10 during the flight. Similar performance also was demonstrated in the laboratory using precision pendulums. For a simplified version which would still meet a spurious acceleration level requirement of less than 1×10^{-12} m/(s^2)/[(Hz)$^{0.5}$] down to 0.1 mHz, it appears that the mass of the entire instrument would be about 10 kg and the volume less than 10^4 cm^3 (Conklin, 2020, private communication).

To make use of the simplified GRSs, the two satellites in the NGGM would need to be flown in a nearly drag free mode of operation. However, for the suggested altitude of 489 km, it appears that the additional mass required to compensate for the non-gravitational forces on the satellites could be accommodated. If the drag is not quite completely compensated for by the thrusters, small known electrical forces can be applied to the test masses to achieve the necessary performance. If nearly drag free operation is considered, there also is the option of flying at lower altitude. However, the resulting increase in sig-

nal level at 50 cycles/rev would be only a factor 3 for 340 km altitude, and this is substantially less than the resulting decrease in total measurement noise due to switching from the use of accelerometers to GRSs.

If simplified versions of the GRSs flown on LISA Pathfinder are not included on the NGGM, an option that has been widely studied in the US is to refly essentially the same type of accelerometers that were flown on GRACE-FO. For this case, we chose to use the expression for the acceleration noise level in the transverse direction given in Table 2 of the paper by Loomis et al. (2012)

$$a = [(1 + 0.005/f)^{0.5}] \times 10^{-7}\mathrm{mm}/(s^2)(Hz^{0.5}) \tag{2}$$

To estimate the noise in the satellite separation, we used the following expression:

$$x_1 = [(2^{0.5})/(2\pi f)^2] \times a \text{ mm}/(\mathrm{Hz}^{0.5}) \tag{3}$$

For both suggested scenarios for the NGGM, we assume that laser ranging interferometry (LRI) would be used to monitor changes in the satellite separation. For the noise due to the laser ranging interferometer measurements between the satellites, we make use of the results reported for the GRACE-FO mission. Early results from the LRI measurements on the GRACE-FO mission have been reported by Abich et al. (2019). At frequencies above 0.1 Hz, the measured displacement noise level shown in Figure 5 agreed with that expected from the frequency noise in the laser, which was tightly locked to a stable reference cavity. At lower frequencies, a curve labeled "laser frequency noise" is shown, which gives the expected displacement noise based on laser frequency noise measurements made before launch. This curve is fit well from 0.3 mHz to 200 mHz by the following expression:

$$x_2 = (2.6 \times 10^{-7})(f^{-0.6})\mathrm{mm}/(\mathrm{Hz}^{0.5}). \tag{4}$$

Then the total instrumental noise level x for measuring the satellite separation is given by the root mean square of x_1 and x_2:

$$x = [(x_1)^2 + (x_2)^2]^{0.5}. \tag{5}$$

To project from the total instrumental noise level at a particular frequency to the corresponding geopotential height variation amplitude requires a short calculation, which is given in the Appendix. This calculation can be regarded as a simplified version of the

approach used by Ghobadi-Far et al. (2018) and others, and does not include the use of correlation-admittance analysis. However, it is expected that it is sufficiently accurate for use in approximate simulations, except at the lowest frequencies. The result is that the expected spectral amplitude of the instrumental noise at a particular frequency should be multiplied by the ratio of the orbital semi-major axis to the satellite separation, which for an altitude of 489 km and an a satellite separation of 220 km is a factor 31.2. In addition, to compare to the results to the expected geophysical geopotential height variations shown in Figures 2 and 3 requires shifting the units for the horizontal axis from $1/(\mathrm{Hz}^{0.5})$ to $1/(\mathrm{cycle/rev})^{0.5}$. For 489 km altitude, this requires dividing the curves by a factor 75.2. Thus the overall correction factor is 0.41.

5 Discussion

If the NGGM is flown at 489 km altitude with simplified GRSs like those discussed above replacing the accelerometers on GRACE-FO, the remaining acceleration noise level would be equal to that from the laser interferometry at about 10 cycles/rev and negligible at substantially higher frequencies. In this case the line-of-sight gravity difference approach could give results over a wide range of frequencies where the uncertainties for individual one revolution arcs would be much lower than the expected signal amplitudes. As a result, even small differences between different procedures for calculating the geopotential height variations based on other types of geophysical data could be detected. This would be an important scientific benefit from using the simplified GRSs on the NGGM. The accuracy for detecting differences between the results for different procedures would be strongly increased. An additional benefit would be to improve the accuracy for measuring the total geopotential variations at the higher frequencies where they become quite small. In particular, for studies of phenomena with short periods like earthquakes (Ghobadi-Far et al., 2019) and tsunamis (Ghobadi-Far et al., 2020) the improved measurement accuracy clearly would be valuable.

It also should be recognized that the reduced acceleration noise would be particularly valuable at high latitudes. There, even very small mass changes at the lower edges of glaciers should be observable with fairly high time resolution. In addition, for the 13-day repeat period orbit geometry considered, there will be a few fairly long arcs which are followed quite closely again in about half a day, but in the opposite direction. Comparing the results for these two arcs would give some statistical information about quite

short period variations in the mass distribution, such as those due to atmospheric wind changes over the oceans.

Curves based on the total instrumental noise level are included in Figures 2 and 3. The top curve for each of the three ground tracks assumes an acceleration noise level for accelerometers like those in the GRACE-FO, as estimated by Loomis et al. (2012), and as given in Eq. 2. The lower curves plotted on Figures 2 and 3 are based on the acceleration noise level with simplified GRSs instead of the accelerometers. The assumed acceleration noise level is $(1\times10^{-12}$ m/s$^2)$/Hz$^{0.5}$ down to 0.1 mHz, as suggested in the first paragraph of Section 4. And for both curves, the laser interferometry noise level discussed in the previous section is assumed.

The advantages of reduced instrumental noise has been pointed out clearly in a recent paper by Landerer et al. (2020) based on the LRI data from the GRACE Follow-On mission during 2019. At the higher frequencies corresponding to spatial resolution of 200 km or better, geopotential features were observed that were not observable in any other type of data. The results were applied particularly in five areas of particular terrestrial water storage anomalies, including areas of significant ice loss over Greenland and Antarctica.

It would be useful to be able to compare the results obtained here for the case of making use of simplified GRSs with results of other studies of possible NGGMs, but that unfortunately usually is not possible because of the quite different assumptions that have been made for different studies. A large number of studies have been carried out in Europe aimed at meeting a specific set of requirements that have been tentatively adopted. A recent paper reports on some of the results from the studies: "ESA's next-generation gravity mission concepts," (Haagmans et al., 2020). However, the main results given are for a quite different mission configuration than we have been considering. Average solutions over seven days have been considered, with satellite altitudes as low as 340 km, and with two pairs of satellites (see e.g., Wiese et al., 2011, 2012). Flying at the lower altitude certainly increases the signal level, particularly at the higher frequencies, but the tradeoffs with the extra requirements for cancelling out the increased drag are under consideration also.

6 Conclusions

Discussions have started in a number of countries of what the scientific requirements should be for a Next Generation Gravity Mission, to follow after the GRACE-FO Mission. In the US, one of the main candidates is a mission like GRACE and GRACE-FO, but with a laser interferometry system like that demonstrated on GRACE-FO relied on to provide high-accuracy measurements of the variations in the satellite separation. However, there are several open issues concerning the mission design. One is whether to fly the mission in a nearly drag-free mode with a fixed ground-track. A second is the altitude to fly at. And a third is whether to replace the accelerometers flown on GRACE and GRACE-FO with simplified versions of the Gravitational Reference Sensors (GRSs) demonstrated very successfully on the LISA Pathfinder Mission.

In most previous comparisons of the expected scientific results with or without the GRSs, it has been assumed that the most valuable results would be those from roughly 10- to 30-day global averages of the geopotential changes from variations in the earth's mass distribution. Other sources of information on those mass changes are used as a priori estimates of the geopotential changes. However, the inaccuracies in the a priori estimates of geopotential changes during the averaging time result in the main limitation on the scientific results from switching to the GRSs.

In this paper an additional way of looking at the benefits of switching to the GRSs is discussed. It is based on our simple approximation to the energy conservation approach. We have chosen the basis for our approach as changes in the satellite separation during one revolution arcs. We used data sets called AOerr and H to represent the estimated uncertainty in the geopotential variations as a function of position and time along 3 quite different one revolution ground tracks and at 3-month intervals. From a comparison of the Fourier transforms of the resulting geopotential variations at satellite altitude with the uncertainty contribution of assumed GRACE-type accelerometers and of laser interferometry between the satellites, the following conclusion was clear: the accelerometer noise very much limited the accuracy with which the geopotential variations along track for each particular arc could be determined, except at low frequencies where limitations due to the orbit determination and analysis approximations would have to be considered. What this means is that the actual geopotential variations could be determined considerably more accurately with the simplified GRSs included. Thus, in addi-

tion to other benefits, differences between different procedures for estimating the geopotential variations from other types of data could be evaluated more precisely.

Appendix A

The purpose of this appendix is to describe the approach that has been used to go from the expected instrumental noise level for determining temporal changes in the satellite separation to what the corresponding errors in the geopotential height variations along the orbit would be. It is assumed that the two satellites follow the same polar orbit, and the rotation of the earth is not considered. The unperturbed along track azimuthal coordinates ϕ_F and ϕ_B for the front and back satellites are assumed to be given by:

$$\phi_F = \omega t + \frac{\gamma}{2} \tag{A1}$$

$$\phi_B = \omega t - \frac{\gamma}{2}. \tag{A2}$$

Here γ is the azimuthal separation of the two satellites, and γ in radians is the nominal satellite separation S divided by R_0, where R_0 is the constant unperturbed orbital radius.

It is assumed that the geopotential height variation is at a single frequency of N cycles per revolution. The resulting perturbed values of the radial and angular coordinates for the front satellite then will be given approximately by the following expressions:

$$R_f = R_0(1+\alpha_r)\ \cos\left[N\omega_0\left(t+\frac{\tau}{2}\right)+\beta_r\right] \tag{A3}$$

$$\phi_f = \omega_0 t + \alpha_\phi\ \cos\left[N\omega_0\left(t+\frac{\tau}{2}\right)+\beta_\phi\right]. \tag{A4}$$

For the back satellite, the coordinates R_b and ϕ_b will be just the same, except with $+\tau/2$ replaced by $-\tau/2$. Here τ is the mean time for a satellite to go the distance S between the satellites:

$$\frac{\tau}{T_0} = \frac{S}{2\pi R_0}, \tag{A5}$$

where T_0 is the orbital period. For 489 km altitude, and $S = 220$ km, $T_0 = 5660$ s, $\omega_0 = 1.11x10^{-3}$ rad/s, and $\tau = 28.9$ s.

From these expressions, the approximate changes in the potential energy and the kinetic energy for the front satellite can be calculated:

$$\delta_{\text{P.E.}} = \frac{gM}{R_f} - \frac{gM}{R_0} = -[\omega_0 R_0]^2 \alpha_r \cos\left[N\omega_0\left(t+\frac{\tau}{2}\right)+\beta_r\right], \tag{A6}$$

$$v_\phi = \omega_0 R_0 - \alpha_\phi R_0 N\omega_0 \sin\left[N\omega_0\left(t+\frac{\tau}{2}\right)+\beta_\phi\right], \tag{A7}$$

$$0.5v_\phi^2 = 0.5\big[\omega_0 R_0\big]^2 - \alpha_\phi\big[R_0\omega_0\big]^2 N \sin\left[N\omega_0\left(t+\frac{\tau}{2}\right)+\beta_\phi\right], \tag{A8}$$

$$\delta_{\text{K.E.}} = -\alpha_\phi\big[R_0\omega_0\big]^2 N \sin\left[N\omega_0\left(t+\frac{\tau}{2}\right)+\beta_\phi\right]. \tag{A9}$$

The sum of $\delta_{\text{P.E.}}$ and $\delta_{\text{K.E.}}$ has to be zero, so:

$$\alpha_r = N\alpha_\phi, \tag{A10}$$

$$\beta_r = \beta_\phi + \frac{\gamma}{2}. \tag{A11}$$

The variations in geopotential height H will be given by $H = \delta_{\text{P.E.}}/{R_0\omega_0}^2$:

$$H = -R_0\alpha_r \cos\left[N\omega_0\left(t+\frac{\tau}{2}\right)+\beta_r\right]. \tag{A12}$$

Thus, from A10 and A11:

$$H = R_0 N\alpha_\phi \sin\left[N\omega_0\left(t+\frac{\tau}{2}\right)+\beta_\phi\right]. \tag{A13}$$

And, since the variations in the satellite separation $R_0(\phi_f - \phi_b)$ are given by A4 and the related expression for ϕ_b,

$$\delta S = (\phi_f - \phi_b)R_0 = -2\alpha_\phi R_0 \sin\big[N\omega_0 t+\beta_\phi\big] \sin\left[N\omega_0\left(\frac{\tau}{2}\right)\right]. \tag{A14}$$

Since $\omega_0(\tau/2) = 0.0160$, even for $N = 100$ the argument of the last sine term is moderate, and thus the last sine term can be approximated roughly by its argument, and:

$$\delta S \sim -N\omega_0\tau\alpha_\phi \sin\big[N\omega_0 t+\beta_\phi\big]. \tag{A15}$$

With the value of τ from A5,

$$\delta S \sim \frac{-NS\omega_0 T_0}{2\pi}\alpha_\phi \sin\big[N\omega_0 t+\beta_\phi\big], \tag{A16}$$

$$\delta S \sim -NS\alpha_\phi \sin\big[N\omega_0 t+\beta_\phi\big]. \tag{A17}$$

From a comparison of A13 and A17, the ratio of the amplitudes for H and δS at the frequency $N\omega_0$ is about R_0/S. There is a phase shift of $N\omega_0\tau/2$ between the two, but this phase difference can be corrected for in the data analysis. Thus the conversion factor from the measured changes in satellite separation to changes in the geopotential height will be approximately a factor R_0/S. For the satellite altitude and separation assumed in this paper, this factor is 31.2.

Acknowledgments

The studies reported in this paper were supported by NASA Award #NNX16AF16G. The data used as the basis for the results shown in Figures 2 and 3 are from the following references: Abich et al. (2019), Dobslaw et al. (2015), and Dobslaw et al. (2016). It is a pleasure to thank David Wiese, Steve Nerem, William Weber, Gerhard Heinzel, John Conklin, Shin-Chan Han, Khosro Ghobadi-Far, and many other scientists interested in satellite gravity measurements for their contributions to this field.

References

Abich, K., Abramovici, A., Amparan, B., Baatzsch, A., Okihiro, B. B., Barr, D. C., ... Zimmermann, M. (2019). In-orbit performance of the GRACE Follow-on laser ranging interferometer. *Physical Review Letters*, *123*(3), 031101. doi: 10.1103/PhysRevLett.123.031101

Armano, M., Audley, H., Baird, J., Binetruy, P., Born, M., Bortoluzzi, D., ... Zweifel, P. (2018). Beyond the required LISA free-fall performance: New LISA pathfinder results down to 20 μHz. *Physical Review Letters*, *120*, 061101. doi: 10.1103/PhysRevLett.120.061101

Conklin, J. R. (2020). Private communication.

Dill, R. (2008). *Hydrological model LSDM for operational Earth rotation and gravity field variations* (Scientific Technical Report No. 08/09). Potsdam: Deutsches GeoForschungsZentrum GFZ. Retrieved from `https://gfzpublic.gfz-potsdam.de/pubman/item/item_8770` doi: 10.2312/GFZ.b103-08095

Ditmar, P., & van Eck van der Sluis, A. A. (2019). A technique for modeling the Earth's gravity field on the basis of satellite accelerations. *Journal of Geodesy*, *78*, 12–33. doi: 10.1007/s00190-003-0362-1

Dobslaw, H., Bergmann-Wolf, I., Dill, R., Forootan, E., Klemann, V., Kusche, J., & Sasgen, I. (2015). The updated ESA Earth System Model for future gravity mission simulation studies. *Journal of Geodesy*, *89*, 505–513. doi: https://doi.org/10.1007/s00190-014-0787-8

Dobslaw, H., Bergmann-Wolf, I., Forootan, E., Dahle, C., Mayer-Gürr, T., Kusche, J., & Flechtner, F. (2016). Modeling of present-day atmosphere and ocean non-tidal de-aliasing errors for future gravity mission simulations. *Journal of Geodesy*, *90*, 423–436. doi: 10.1007/s00190-015-0884-3

Flechtner, F., Neumayer, K.-H., Dahle, C., Dobslaw, H., Fagiolini, E., Raimondo, J.-C., & Güntner, A. (2016). What can be expected from the GRACE-FO laser ranging interferometer for Earth science applications? *Surveys in Geophysics 37*, *2*, 453–470. doi: 10.1007/s10712-015-9338-y

Ghobadi-Far, K., Han, S.-C., Allgeyer, S., Tregoning, P., Sauber, J., Behzadpour, S., ... Okal, E. (2020). GRACE gravitational measurements of tsunamis after the 2004, 2010, and 2011 great earthquakes. *Journal of Geodesy*, *944*, 65. doi: https://doi.org/10.1007/s00190-020-01395-3

Ghobadi-Far, K., Han, S.-C., Sauber, J., Lemoine, F., Behzadpour, S., Mayer-Gürr, T., ... Okal, E. (2019). Gravitational changes of the Earth's free oscillation from earthquakes: Theory and feasibility study using GRACE inter-satellite tracking. *Journal of Geophysical Research: Solid Earth*, *124*(7), 7483–7503. doi: https://doi.org/10.1029/2019JB017530

Ghobadi-Far, K., Han, S.-C., Weller, S., Loomis, B. D., Luthcke, S. C., Mayer-Gürr, T., & Behzadpour, S. (2018). A transfer function between line-of-sight gravity difference and GRACE intersatellite ranging data and an application to hydrological surface mass variation. *Journal of Geophysical Research: Solid Earth*, *123*(10), 9186–9201. doi: https://doi.org/10.1029/2018JB016088

Haagmans, R., Siemes, C., Massotti, L., Carraz, O., & Silvestrin, P. (2020). ESAs next-generation gravity mission concepts. *Rendiconti Lincie. Scienze Fisiche e Naturali*. doi: https://doi.org/10.1007/s12210-020-00875-0

Han, S.-C. (2004). Efficient determination of global gravity field from satellite-to-satelite tracking mission. *Celestial Mechanics and Dynamical Astronomy*, *88*, 69–102. doi: https://doi.org/10.1023/B:CELE.0000009383.07092.1f

Han, S.-C., Shum, C. K., & Jekeli, C. (2006). Precise estimation of in situ geopotential differences from GRACE low-low satellite-to-satellite tracking and accelerometer data. *Journal of Geophysical Research*, *111*(B4), 1–13. doi: https://doi.org/10.1029/2005JB003719

Han, S.-C., Shum, C. K., Jekeli, C., & Alsdorf, D. (2005). Improved estimation of terrestrial water storage changes from GRACE. *Geophysical Research Letters*, *32*, L07302. doi: https://doi.org/10.1029/2005GL022382

Jekeli, C. (1999). The determination of gravitational potential differences from satellite-to-satellite tracking. *Celestial Mechanics and Dynamical Astronomy*,

75(2), 85–101. doi: https://doi.org/10.1023/A:1008313405488

Jekeli, C. (2017). The energy balance approach. In M. Naeimi & J. Flury (Eds.), *Global Gravity Field Modeling from Satellite-to-Satellite Tracking Data* (pp. 127–160). Switzerland: Springer, Cham. doi: https://doi.org/10.1007/978-3-319-49941-3

Kornfeld, R. P., Arnold, B. W., Gross, M. A., Dahya, N. T., & Klipstein, W. M. (2019). GRACE-FO: The Gravity Recovery and Climate Experiment Follow-On mission. *Journal of Spacecraft and Rockets*, *56*(3), 931–951. doi: https://doi.org/10.2514/1.A34326

Landerer, F. W., Flechtner, F. M., Save, H., Webb, F. H., Bandikova, T., Bertiger, W. I., ... Yuan, D.-N. (2020). Extending the global mass change data record: GRACE Follow-On instrument and science data performance. *Geophysical Research Letters*, *47*(12), e2020GL088306. doi: https://doi.org/10.1029/2020GL088306

Loomis, B. D., Nerem, R. S., & Luthcke, S. B. (2012). Simulation study of a follow-on gravity mission to GRACE. *Journal of Geodesy*, *86*(5), 319–335. doi: https://doi.org/10.1007/s00190-011-0521-8

Tapley, B. D., Bettadpur, S., Watkins, M., & Reigber, C. (2004). he gravity recovery and climate experiment, mission overview and early results. *Geophysical Research Letters*, *31*(9), L09607. doi: https://doi.org/10.1029/2004GL019920

Tapley, B. D., Watkins, M. M., Flechtner, F., Reigber, C., Bettadpur, S., Rodell, M., ... Velicogna, I. (2019). Contributions of grace to understanding climate change. *Nature Climate Change*, *9*, 358–369. doi: https://doi.org/10.1038/s41558-019-0456-2

Watkins, M., Wiese, D. N., Yuan, D.-N., Boening, C., & Landerer, F. W. (2015). Improved methods for observing earth's time variable mass distribution with grace using spherical cap mascons. *Journal of Geophysical Research: Solid Earth*, *120*, 2648–2671. doi: https://doi.org/10.1002/2014JB011547

Weigelt, M. (2017). The acceleration approach. In M. Naeimi & J. Flury (Eds.), *Global Gravity Field Modeling from Satellite-to-Satellite Tracking Data* (pp. 97–126). Switzerland: Springer, Cham. doi: https://doi.org/10.1007/978-3-319-49941-3

Wiese, D. N., Nerem, R. S., & Han, S.-C. (2011). Expected improvements in de-

termining continental hydrology, ice mass variations, ocean bottom pressure signals, and earthquakes using two pairs of dedicated satellites for temporal gravity recovery. *Journal of Geophysical Research*, *116*, B11405. doi: https://doi.org/10.1029/2011JB008375

Wiese, D. N., Nerem, R. S., & Lemoine, F. G. (2012). Design considerations for a dedicated gravity recovery satellitemission consisting of two pairs of satellites. *Journal of Geodesy*, *86*, 81–98. doi: https://doi.org/10.1007/s00190-011-0493-8

Wolff, M. (1969). Direct measurement of the Earth's gravitational potential using a satellite pair. *Journal of Geophysical Research*, *74*(22), 5295–5300. doi: https://doi.org/10.1029/JB074i022p05295

Figure 1.

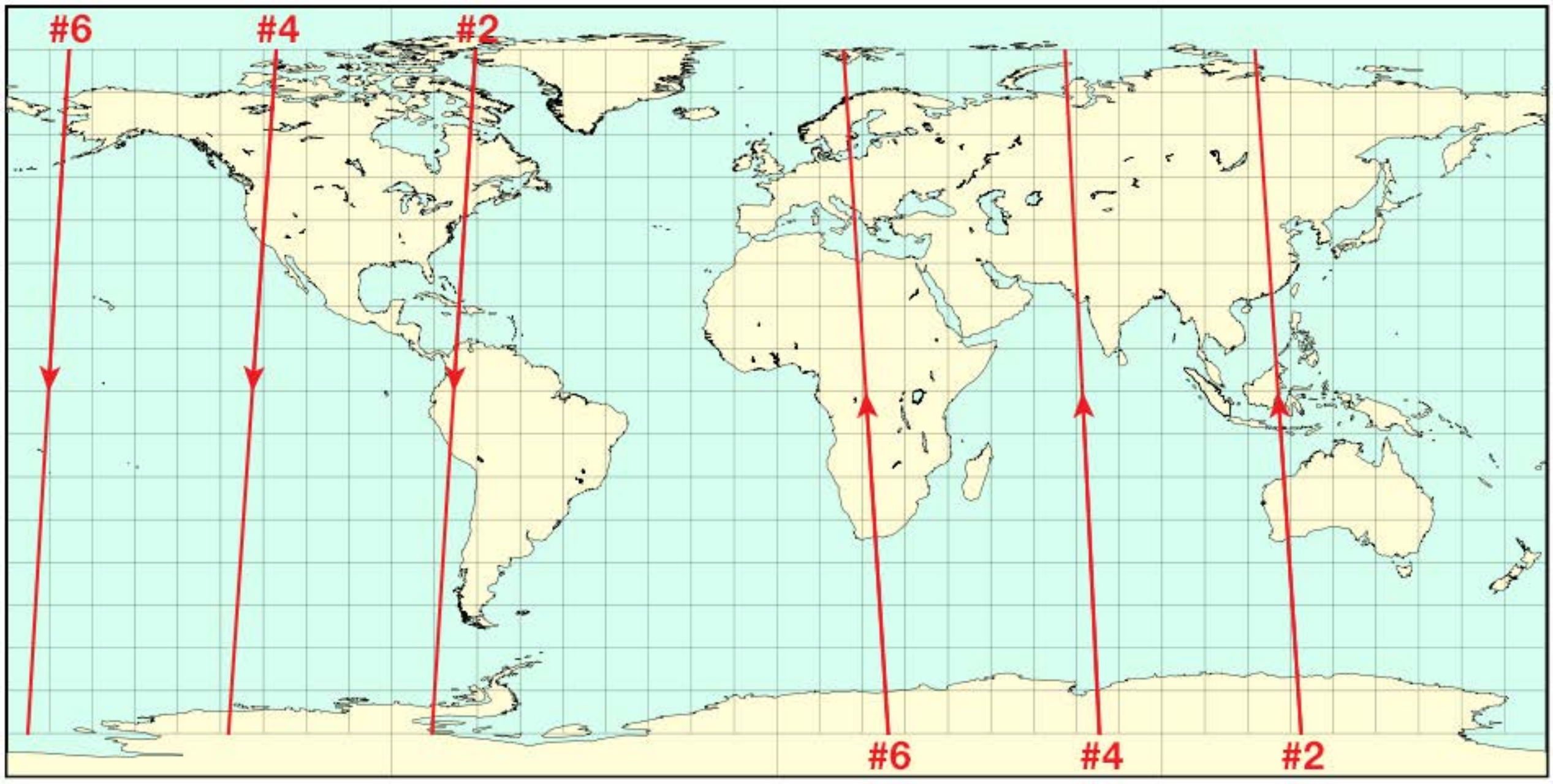
#6
#4
#2
#6
#4
#2

Figure 2.

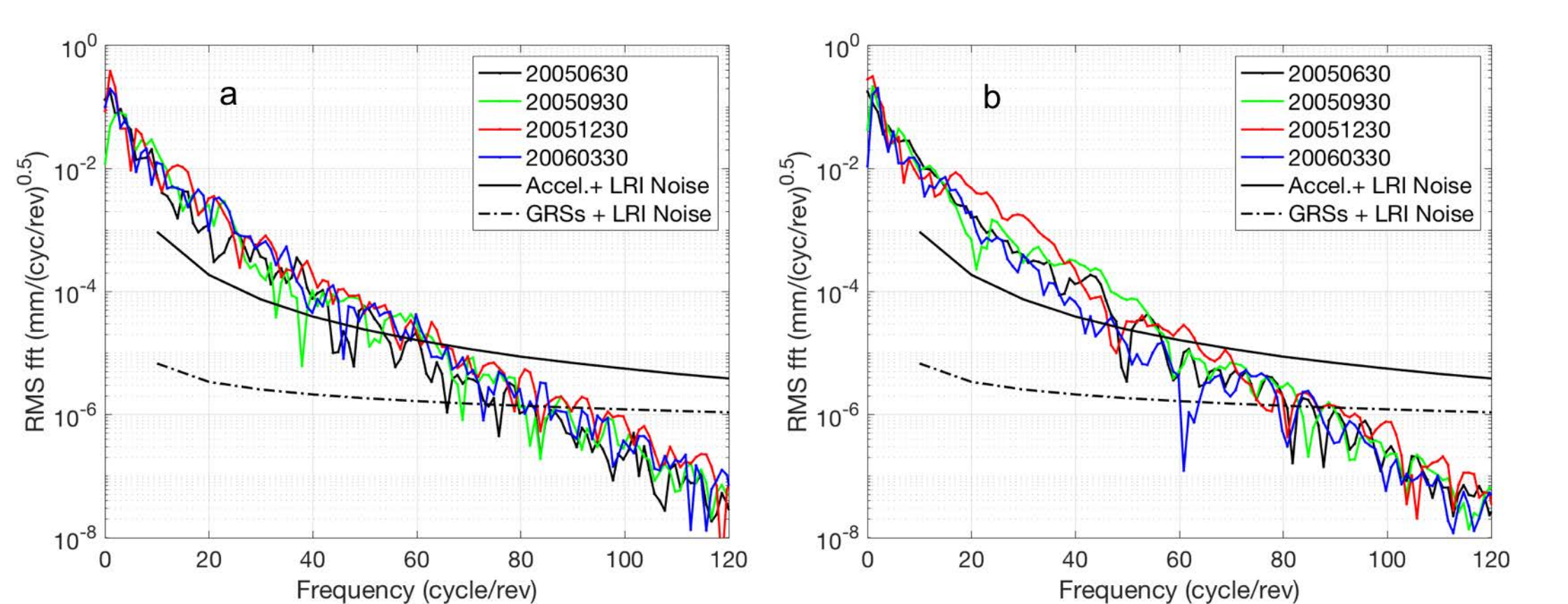
a
b
20050630
20050930
20051230
20060330
Accel.+ LRI Noise
GRSs + LRI Noise
RMS fft (mm/(cyc/rev)^0.5)
Frequency (cycle/rev)
10^0
10^-2
10^-4
10^-6
10^-8
0
20
40
60
80
100
120

Figure 3.

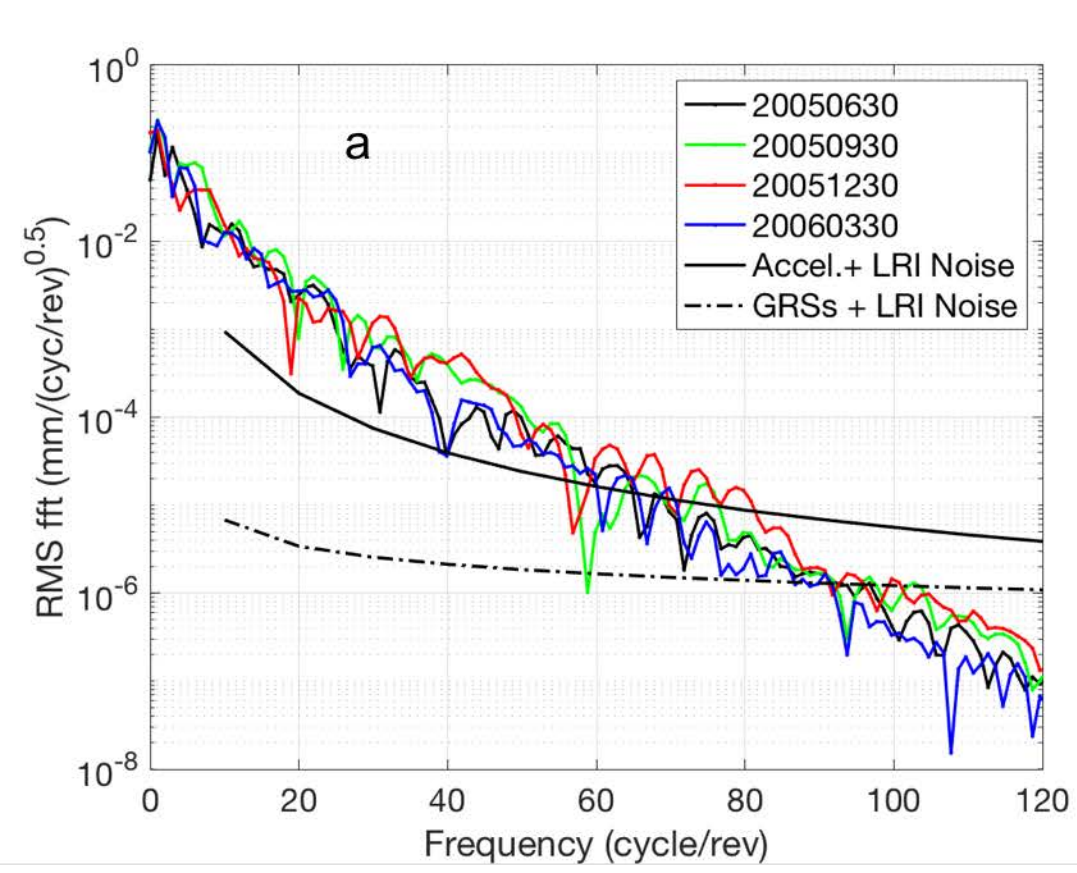
a
20050630
20050930
20051230
20060330
Accel.+ LRI Noise
GRSs + LRI Noise
RMS fft (mm/(cyc/rev)^0.5)
Frequency (cycle/rev)

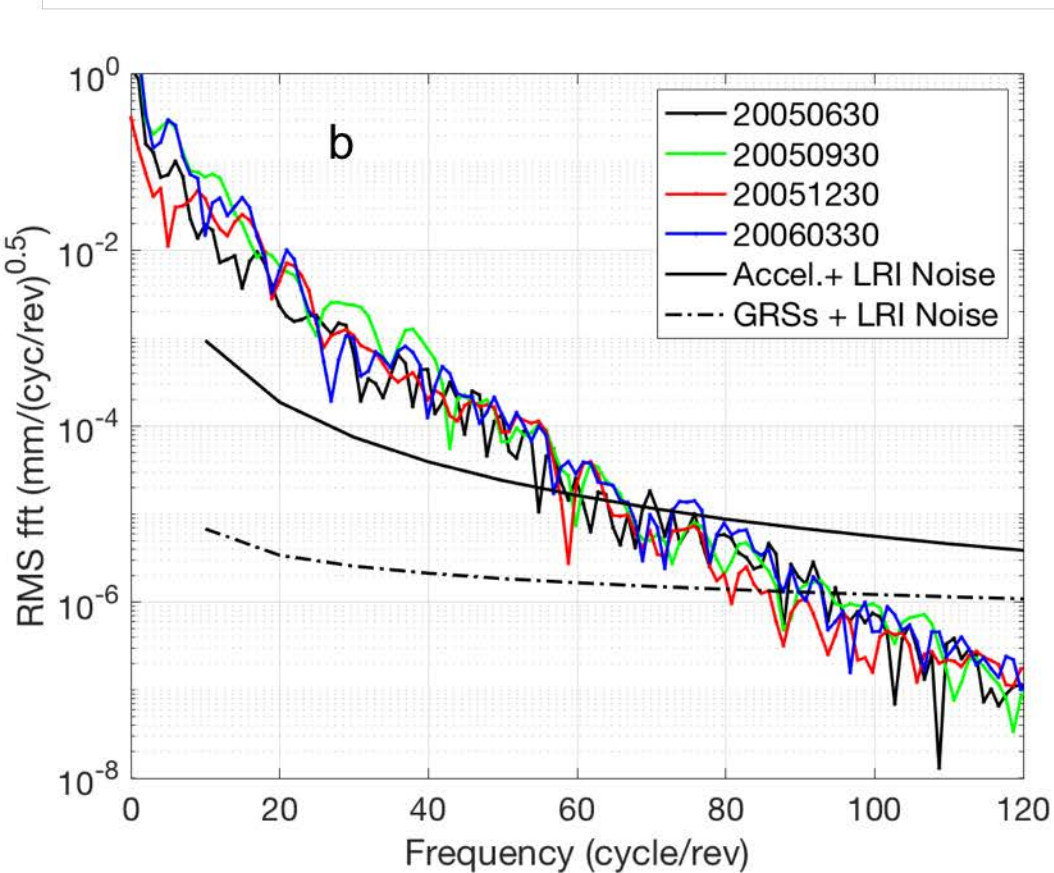
b
20050630
20050930
20051230
20060330
Accel.+ LRI Noise
GRSs + LRI Noise
RMS fft (mm/(cyc/rev)^0.5)
Frequency (cycle/rev)